

DETERMINATION OF KINETIC PARAMETERS FOR THE THERMAL DECOMPOSITION OF PHENOLIC ABLATIVE MATERIALS BY A MULTIPLE HEATING RATE METHOD

J.B. HENDERSON, M.R. TANT and G.R. MOORE

Naval Surface Weapons Center, Dahlgren, VA 22448 (U.S.A.)

J.A. WIEBELT

School of Mechanical and Aerospace Engineering, Oklahoma State University, Stillwater, OK 74074 (U.S.A.)

(Received 1 July 1980)

ABSTRACT

The rate of decomposition for two widely used glass- and asbestos-phenolic ablative materials were measured using standard thermogravimetric techniques. Thermograms were obtained at six heating rates ranging from $10^{\circ}\text{C min}^{-1}$ to $160^{\circ}\text{C min}^{-1}$. From these data the kinetic parameters were determined by a slightly modified version of Friedman's method. Fractional weight loss calculated using the derived kinetic parameters over the temperature range of decomposition agreed with measured values with a mean error of 0.33 and 0.28%, with a standard deviation of errors 0.58 and 0.84% for glass- and asbestos-phenolic, respectively. The 95% confidence for the mean error was 0.22 and 0.44% for the glass-phenolic and 0.14 and 0.42% for the asbestos-phenolic. Also, the activation energy was calculated by the method of Flynn and Wall. The average activation energy values determined by the two methods agreed within 4.6% for both materials.

INTRODUCTION

The rate of decomposition of an ablative material when heated is modeled by the kinetic rate equation. If it is assumed that the material dimensions are constant, the rate equation determines the density of the remaining char. Both the rate of decomposition and char density strongly affect the thermal performance of the material. In order to predict the thermal response, accurate values of the kinetic parameters over the entire range of decomposition are required. For the case of an ablative material exposed to a solid rocket motor exhaust, the heat flux may vary widely depending upon the geometry and/or type of motor. Therefore, the effect of the heating rate on the kinetic parameters must also be known.

The purpose of this study was to determine an appropriate model for the rate of decomposition of ablative materials. Friedman's method [1] using multiple heating rates was chosen since ablative materials are subjected to widely varying heating rates. Application of this method required calculating an average activation energy for the entire thermal decomposition. The

decomposition reaction required two models, one for the initial decomposition and another for the remainder. For these two regions separate pre-exponential factors and apparent orders of reaction were calculated by the technique developed by Friedman [1]. For comparison the average activation energy for each material determined by Friedman's method was compared to the value obtained by the method of Flynn and Wall [2].

PREVIOUS WORK

The decomposition kinetics of solid materials have been studied by many investigators. As a result, numerous techniques have been developed to extract the kinetic parameters from experimental data.

Freeman and Carroll [3] developed the well-known difference method and applied the technique to determine the kinetic parameters for calcium oxalate monohydrate. The method was later revised by Anderson and Freeman [4] and applied to the study of polystyrene and polyethylene. Mickelson and Einhorn [5] developed the ratio method to analyze thermogravimetric data obtained for a urethane polymer. Baer et al. [6] heated samples of reinforced polymers at heating rates up to $4200^{\circ}\text{C min}^{-1}$. The data were correlated by a numerical technique developed by Burningham and Seader [7]. Friedman [1] studied the decomposition of a fiberglass-phenolic based on a technique developed for multiple heating rates. Similarly, Flynn and Wall [2] developed a method for determining the activation energy based on data taken at several different heating rates.

Baer et al. [6] discussed the fact that kinetic parameters obtained by methods using a single thermogram at low heating rates do not accurately predict kinetic behavior when applied to the higher heating rates. For this reason the methods of Friedman [1] and Flynn and Wall [2] were considered in this work.

THEORY

Friedman's method

Friedman's method is attractive for this application because the kinetic properties may be calculated based on data taken over a wide range of heating rates. Further, the Arrhenius equation is combined with an arbitrary function of weight. This allows more flexibility, since no prior knowledge of the function is required. This method does, however, require measurement of the weight loss and rate of weight loss as a function of temperature, at several different heating rates.

The general form of the rate equation proposed by Friedman is

$$-1/W_0 \times dW/dt = Af(W/W_0) \exp(-E/RT) \quad (1)$$

where W_0 = original weight of material (mg), dW/dt = rate of weight loss (mg min^{-1}), A = pre-exponential factor (min^{-1}), E = activation energy (cal g

mole⁻¹), R = gas constant (1.987 cal g-mole⁻¹ K⁻¹), T = temperature (K), and $f(W/W_0)$ = undefined function of weight.

Taking the natural logarithm of both sides of eqn. (1) results in

$$\ln[-1/W_0 \times dW/dt] = \ln[Af(W/W_0)] - E/RT \quad (2)$$

A linear equation may be fit to $\ln[-1/W_0 \times dW/dt]$ as a function of $1/T$ at constant parametric values of W/W_0 . These equations will have slopes of $-E/R$. Each intercept is the value of $\ln[Af(W/W_0)]$ at the parametric value of W/W_0 . Then by defining

$$f(W/W_0) = [(W - W_f)/W_0]^n \quad (3)$$

where n = order of reaction, W = instantaneous weight of material (mg), W_f = final weight of charred material (mg), and multiplying eqn. (3) by A and taking the natural logarithm results in

$$\ln[Af(W/W_0)] = \ln A + n \ln[(W - W_f)/W_0] \quad (4)$$

The final ratio, W_f/W_0 , is taken from the original thermograms. Since $\ln[Af(W/W_0)]$ is known for various W/W_0 ratios, eqn. (4) can be used to obtain values of A and n .

Discussion of Friedman's technique

Friedman used this technique to calculate the kinetic properties for CTL91-LD fiberglass-phenolic. One activation energy was calculated for each of the 12 values of weight loss ranging from 0.675 to 0.95 (on a glass-free basis). The average activation energy was calculated from these data. By eliminating the early weight loss ($\approx 4\%$) and dropping the data points above $W/W_0 = 0.875$ and using $W_f/W_0 = 0.61$, a linear curve was fit to the data. Thus the effective range covered by the curve fit was approximately $0.65 \leq W/W_0 \leq 0.85$, which accounted for about 50% of the total weight loss. This resulted in a rather poor fit of the data at both ends of the weight loss curve. In contrast, the requirement for the present application was to obtain a kinetic expression applicable over the entire range of weight loss.

Three points regarding this method should be clarified. First, the equation of $f(W/W_0)$ may take a variety of forms. For example, Goldfarb et al. [8] selected $f(W/W_0) = [(W - W_f)/(W_0 - W_f)]^n$. This should result only in a change in the intercept $\ln A$, i.e. a change in the apparent pre-exponential factor.

Secondly, the kinetic parameters may be calculated by considering the total weight or only the resin weight of the sample. Again the activation energy and order of reaction remain unchanged. Only the intercept $\ln A$ is affected.

Using a pre-exponential factor based only on the resin weight will result in an error if used in calculations where the total weight is being considered. Assuming the unknown function is $[(W - W_f)/W_0]^n$, the two pre-exponential factors are related by

$$A' = A[(W_0 - W_g)/W_0]^{n-1} \quad (5)$$

where A' = pre-exponential factor (resin weight only) (min^{-1}), and W_g = weight of inert material (mg).

Finally, changes in the activation energy at different degrees of conversion may be a result of real changes due to a change in mechanism or a change in structure of the resin or a result of experimental error. If these changes are not a result of experimental error, then using $E = E(W/W_0)$ would be more realistic. In many cases, however, separation of the experimental error from real changes in E is difficult.

Flynn and Wall's method

Flynn and Wall [2] developed a convenient method to determine the activation energy from weight loss curves measured at several heating rates. The following relationship is used to calculate the activation energy.

$$E \approx -(R/C) d \log \beta / d(1/T) \quad (6)$$

where β = heating rate ($^{\circ}\text{C min}^{-1}$), and $C = C(E/RT)$.

Plotting $1/T$ vs. $\log \beta$ at several weight loss ratios results in a series of straight lines with slope $\Delta \log \beta / \Delta(1/T)$. Using the slope and the appropriate value of C , the activation energy can be calculated by eqn. (6). Since C is a function of E/RT , calculation of E from eqn. (6) is an iterative process. Flynn and Wall constructed a table of values for C over a range of values of $7 \leq E/RT \leq 60$. The variation of C over this range is approximately $\pm 3\%$. This method is extremely attractive since it involves only reading the temperature at a constant weight loss from a series of thermograms at different heating rates.

EXPERIMENTAL

Materials

The two ablative materials studied were supplied by Haveg Industries. As shown in Table 1, these materials consisted of a phenol-formaldehyde resin with specified amounts of glass, asbestos, and/or magnesium silicate added as

TABLE 1

Composition of materials tested

Contents	Material composition (%)	
	H41NE	H41D
Asbestos		52.0
Glass (SiO_2) and talc (Mg_2SiO_4)	60.5	
Total filler content	60.5	52.0
Phenol-formaldehyde resin (H41P)	39.5	48.0
Total nonvolatiles	60.5	52.0

filler. The materials were converted to powder form by machining and were then filtered through a No. 20 sieve. They were stored overnight in a vacuum desiccator maintained at 35°C to remove traces of water.

Apparatus and procedure

A Perkin-Elmer TGS-2 Thermogravimetric System was used, with temperature control provided by a Perkin-Elmer System 4 Microprocessor Controller. The sample temperature was measured with a chromel—alumel thermocouple which was calibrated with a set of five Curie standards in the temperature range of interest at each heating rate used [9].

In order to reduce temperature gradients in the material and to ensure uniform heating, small weights of a powdered form of the materials were used. Samples weighing 7.5 ± 0.5 mg were heated from 40°C to 950°C using heating rates of 10, 20, 40, 80, 100, and 160°C min⁻¹. Both the percentage of initial weight and the rate of weight loss were plotted directly as a function of temperature. The samples were maintained in a nitrogen atmosphere throughout the experiment. When the programmed temperature scan reached 950°C, the purge gas was automatically switched to oxygen to thermo-oxidatively degrade the remaining resin. To verify the initial weight fraction of filler, the temperature was held at 950°C until the resin had completely degraded.

RESULTS

The original thermograms contained the temperature, derivative of weight loss and the fraction of weight remaining. These data were digitized at 0.01

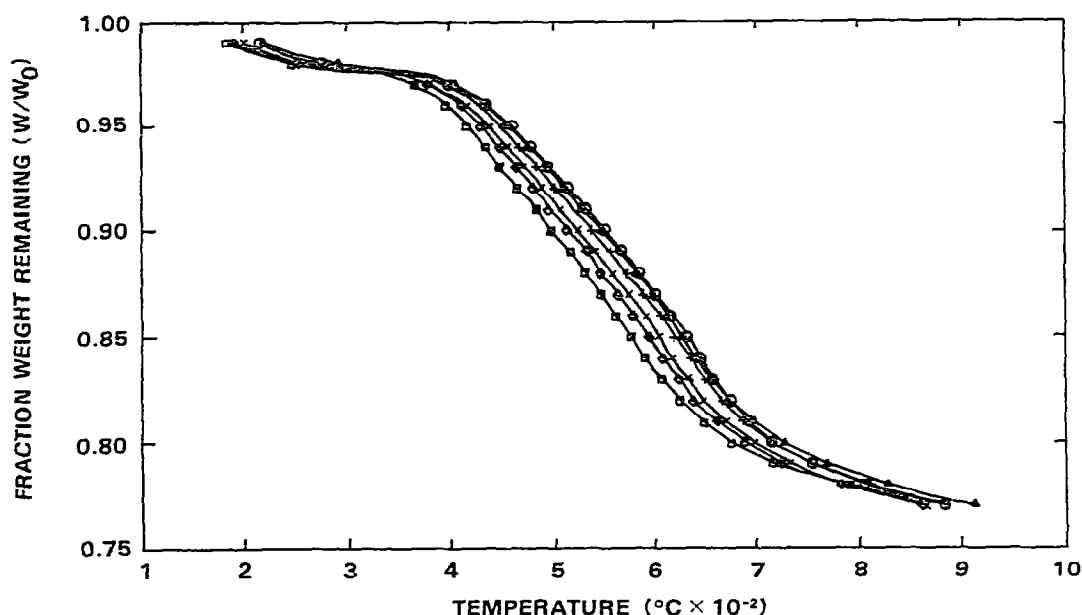


Fig. 1. Fraction weight remaining for all six heating rates for H41D. □, 10°C min⁻¹; ◇, 20°C min⁻¹; ×, 40°C min⁻¹; +, 80°C min⁻¹; ▲, 100°C min⁻¹; ○, 160°C min⁻¹.

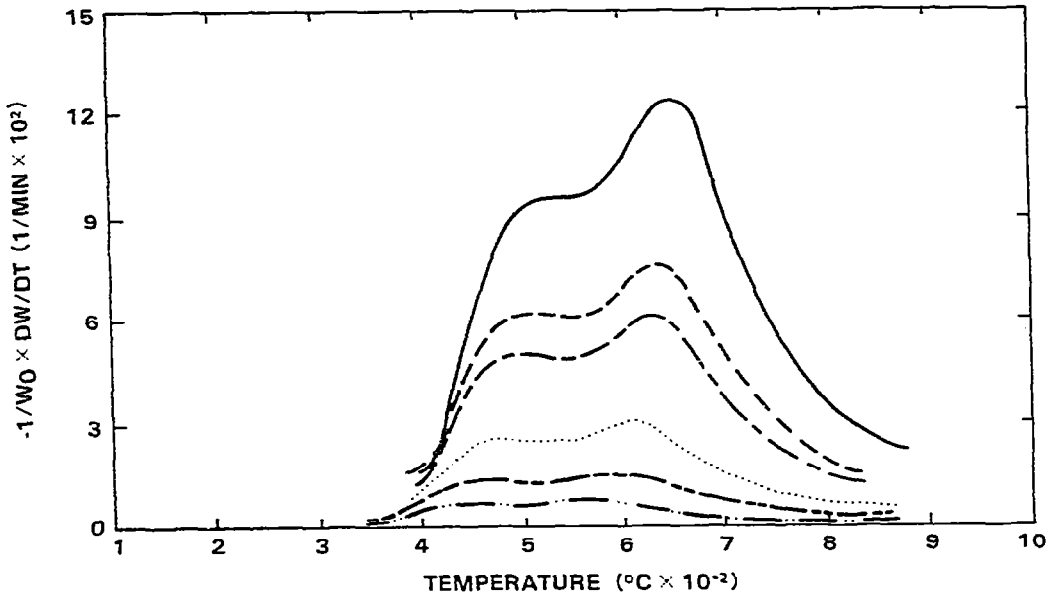


Fig. 2. Derivative of weight loss for all six heating rates for H41D. ---, 10°C min⁻¹; - - - -, 20°C min⁻¹; ·····, 40°C min⁻¹; - - - -, 80°C min⁻¹; - - - -, 100°C min⁻¹; ———, 160°C min⁻¹.

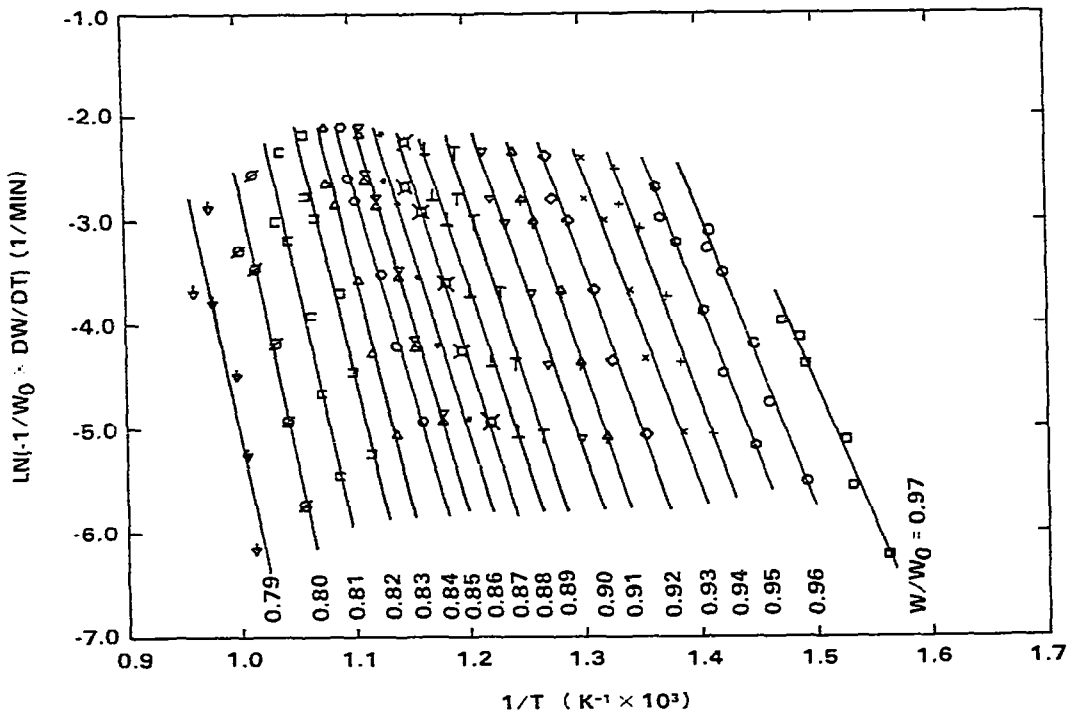


Fig. 3. Plot of slopes used to determine activation energy for H41D. $0.79 \leq W/W_0 \leq 0.97$.

TABLE 2
Experimental data

W/W_0	Heating rate 160°C min ⁻¹			Heating rate 100°C min ⁻¹			Heating rate 80°C min ⁻¹		
	H41NE $W_0 = 7.9306$	H41D $W_0 = 7.3061$	H41NE $W_0 = 7.4272$	H41D $W_0 = 7.8094$	H41NE $W_0 = 7.8858$	H41D $W_0 = 7.0392$			
	T (°C)	$(-1/W_0) \times$ (dW/dt) (min ⁻¹)	T (°C)	$(-1/W_0) \times$ (dW/dt) (min ⁻¹)	T (°C)	$(-1/W_0) \times$ (dW/dt) (min ⁻¹)	T (°C)	$(-1/W_0) \times$ (dW/dt) (min ⁻¹)	
0.98	403.0	0.0203	390.0	0.0106	400.0	0.0151	400.0	0.0151	
0.97	436.0	0.0496	432.3	0.0312	407.1	0.0190	430.0	0.0304	
0.96	460.0	0.0688	454.9	0.0436	437.7	0.0385	452.0	0.0384	
0.95	480.0	0.0786	476.5	0.0498	459.2	0.0507	472.0	0.0413	
0.94	500.0	0.0827	497.1	0.0517	478.6	0.0580	492.0	0.0415	
0.93	521.0	0.0815	497.0	0.0913	495.9	0.0618	514.0	0.0393	
0.92	544.0	0.0773	516.0	0.0944	513.3	0.0618	539.0	0.0378	
0.91	566.0	0.0773	534.0	0.0958	529.6	0.0608	561.0	0.0382	
0.90	586.0	0.0808	552.0	0.0958	548.0	0.0607	581.0	0.0413	
0.89	605.8	0.0866	568.0	0.0965	567.4	0.0616	602.9	0.0445	
0.88	623.5	0.0922	587.0	0.1010	582.7	0.0645	620.7	0.0465	
0.87	640.3	0.0953	601.0	0.1063	600.0	0.0691	639.5	0.0462	
0.86	659.0	0.0934	616.7	0.1143	613.9	0.0731	659.3	0.0426	
0.85	676.7	0.0831	632.4	0.1196	627.8	0.0759	686.0	0.0332	
0.84	705.2	0.0657	645.2	0.1230	640.8	0.0755	720.6	0.0259	
0.83			658.0	0.1224	656.7	0.0718	649.5	0.0581	
0.82			674.7	0.1150	672.6	0.0639	665.7	0.0519	
0.81			692.4	0.0983	697.5	0.0501	686.9	0.0418	
0.80			715.1	0.0787	727.3	0.0379	714.2	0.0317	
0.79			753.5	0.0560	768.1	0.0250	751.6	0.0224	

TABLE 2 (continued)

W/W ₀	Heating rate 40°C min ⁻¹			Heating rate 20°C min ⁻¹			Heating rate 10°C min ⁻¹			
	H41NE W ₀ = 7.6769	H41D W ₀ = 7.9664	H41NE W ₀ = 7.1357	H41D W ₀ = 7.5368	H41NE W ₀ = 7.4106	H41D W ₀ = 7.6958				
	T (°C)	(-1/W ₀) × (dW/dt) (min ⁻¹)	T (°C)	(-1/W ₀) × (dW/dt) (min ⁻¹)	T (°C)	(-1/W ₀) × (dW/dt) (min ⁻¹)	T (°C)	(-1/W ₀) × (dW/dt) (min ⁻¹)	T (°C)	(-1/W ₀) × (dW/dt) (min ⁻¹)
0.98	371.7	0.0051	370.6	0.0042	363.3	0.0026	367.1	0.0019		
0.97	412.2	0.0146	398.6	0.0083	380.6	0.0038	392.0	0.0047	367.1	0.0019
0.96	437.1	0.0195	423.6	0.0105	412.4	0.0086	415.6	0.0059	397.4	0.0040
0.95	456.9	0.0215	441.2	0.0112	431.9	0.0114	430.0	0.0062	418.6	0.0057
0.94	479.7	0.0215	460.9	0.0110	450.3	0.0127	452.5	0.0061	436.7	0.0064
0.93	495.3	0.0203	474.0	0.0254	466.7	0.0131	469.9	0.0058	449.8	0.0065
0.92	521.2	0.0191	491.4	0.0255	483.1	0.0130	492.5	0.0054	467.0	0.0064
0.91	542.0	0.0193	508.8	0.0250	498.5	0.0126	514.0	0.0054	486.1	0.0062
0.90	563.8	0.0206	525.2	0.0245	516.0	0.0123	531.4	0.0058	499.2	0.0061
0.89	584.6	0.0223	542.7	0.0246	534.4	0.0125	556.0	0.0062	519.4	0.0062
0.88	604.1	0.0234	561.1	0.0256	548.8	0.0131	571.4	0.0063	533.5	0.0066
0.87	621.3	0.0236	575.5	0.0274	566.2	0.0142	591.9	0.0063	549.7	0.0071
0.86	640.5	0.0221	592.9	0.0291	580.6	0.0149	612.8	0.0054	562.8	0.0074
0.85	655.7	0.0176	605.8	0.0303	595.9	0.0154	635.6	0.0049	577.9	0.0075
0.84	698.1	0.0140	617.5	0.0299	608.7	0.0150	668.2	0.0038	591.0	0.0073
0.83			634.2	0.0281	625.1	0.0138			608.4	0.0064
0.82			647.9	0.0247	638.7	0.0118			626.8	0.0053
0.81			670.4	0.0201	661.9	0.0096			649.1	0.0043
0.80			697.8	0.0154	689.0	0.0073			676.2	0.0032
0.79			732.1	0.0112	722.9	0.0052			715.9	0.0021

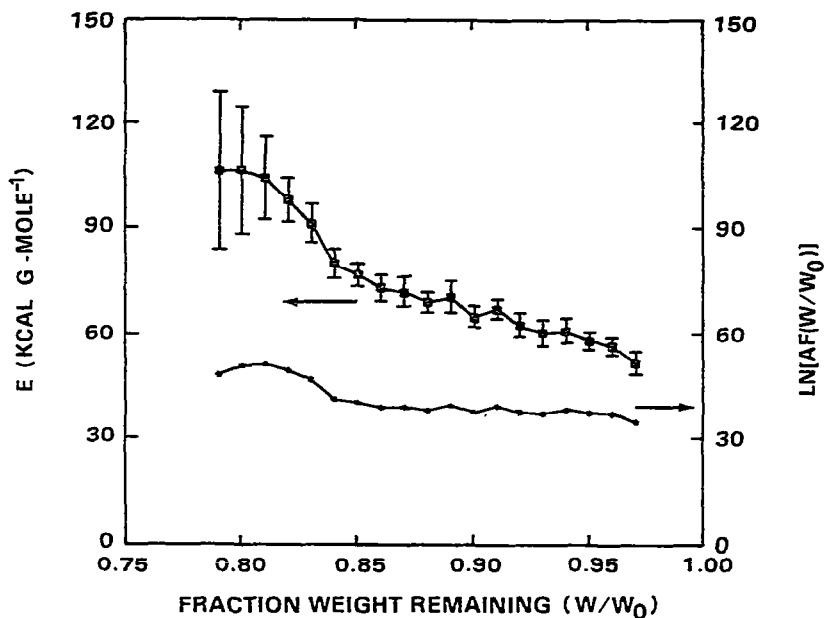


Fig. 4. Activation energy and intercept as a function of degree of conversion for H41D. $E_{ave} = 74.97 \text{ kcal g-mole}^{-1}$.

intervals of the fraction of weight remaining. The experimental temperatures were corrected using the Curie standard temperature calibration for each heating rate. The thermograms were reproduced from these data. Comparison of the fraction of weight remaining and the derivative of weight loss as a function of temperature at all six heating rates for H41D is shown in Figs. 1

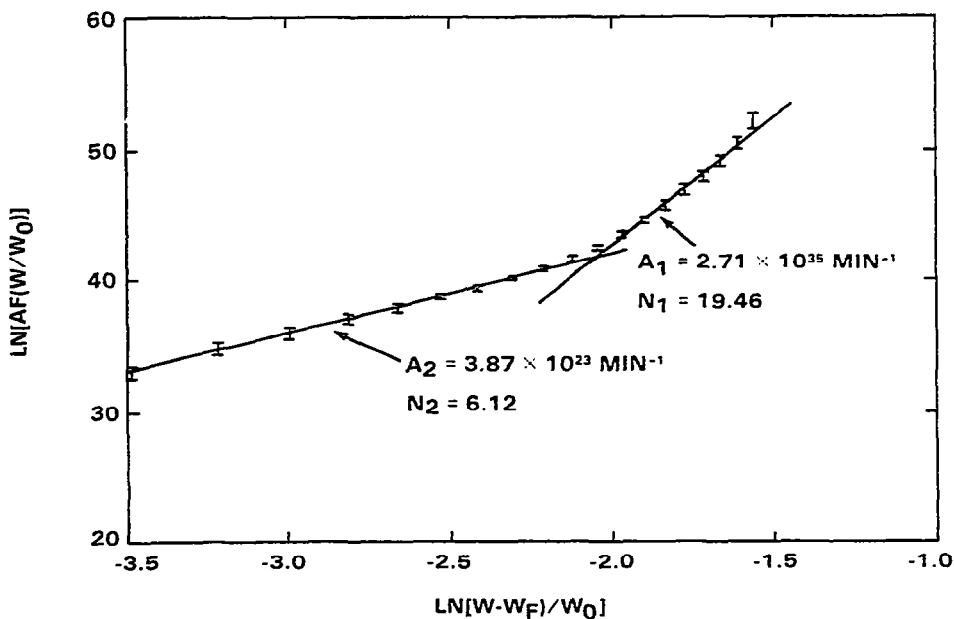


Fig. 5. Plot to determine the pre-exponential factor and order of reaction for two regions of weight loss for H41D.

TABLE 3

Summary of calculations

Material	W_f/W_0	Range of W/W_0	$E_{ave.}(\text{kcal g-mole}^{-1})$		$A (\text{min}^{-1})$	n	W/W_0
			Friedman	Flynn and Wall			
H41Ne	0.795	0.98—0.84	62.13	62.15	1.19×10^{31}	17.33	≥ 0.91
					4.90×10^{20}	6.30	< 0.91
H41D	0.760	0.97—0.79	74.97	71.52	2.71×10^{35}	19.46	≥ 0.89
					3.87×10^{23}	6.12	< 0.89

and 2, respectively. The digitized data for both materials is listed in Table 2.

A plot of $\ln[-1/W_0 \times dW/dt]$ vs. $1/T$ for H41D is shown in Fig. 3. The slope of each line was determined from a least squares fit of the data. Figure 4 shows the corresponding activation energy and intercept $\ln[Af(W/W_0)]$ at each value of weight loss from $0.79 \leq W/W_0 \leq 0.97$. The range of each data point is the range of error based on the least squares fit of the data. Values of $\ln[Af(W/W_0)]$ vs. $\ln[(W - W_f)/W_0]$ for H41D are shown in Fig. 5. This figure depicts the separation of the reaction into the two regions and the corresponding least squares fit over each region. A pre-exponential factor and order of reaction were determined for each of these two regions. The average activation energy determined from Fig. 3 was used for both regions. Using Flynn and Wall's method, the average activation energies for both

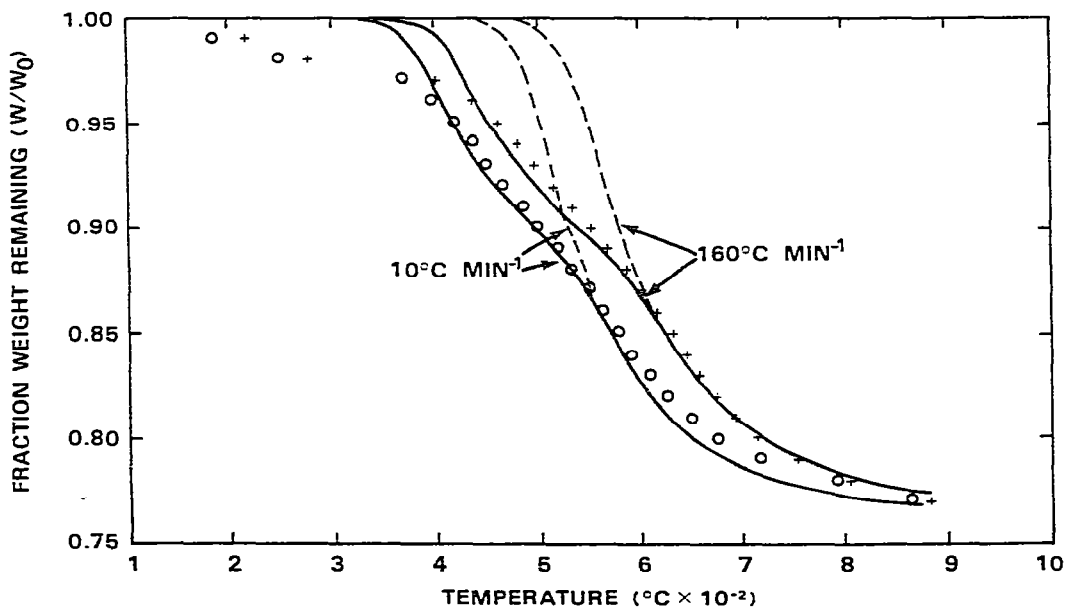


Fig. 6. Comparison of calculated vs. experimental weight loss curves for H41D at $10^\circ\text{C min}^{-1}$ and $160^\circ\text{C min}^{-1}$ heating rates. —, Present work; ---, previous method; +, o, experimental.

TABLE 4

Statistical analysis of errors in computed vs. experimental W/W_0

Material	Aver. error (%)	S.D. (%)	95% Confidence interval (%)
H41NE	0.33	0.58	0.22—0.44
H41D	0.28	0.84	0.14—0.42

materials were calculated based on plots of $\log \beta$ vs. $1/T$. A summary of the results of the calculations for both materials is listed in Table 3.

The kinetic parameters calculated by the modified version of Friedman's method were used in eqn. (1) to calculate the fraction of weight remaining vs. temperature. Each set of parameters was applied to that portion of the weight loss curve from which it was determined. A comparison of the results of these calculations and the experimental data for $10^\circ\text{C min}^{-1}$ and $160^\circ\text{C min}^{-1}$ heating rates for H41D are shown in Fig. 6. The average error, standard deviation of errors and the 95% confidence interval were calculated for 90 and 114 experimental vs. calculated points for H41NE and H41D, respectively. The results are presented in Table 4.

DISCUSSION

The average activation energies calculated by the methods of Flynn and Wall and Friedman agree within 0.03 and 4.6% for H41NE and H41D, respectively. There was less scatter of the data using Flynn and Wall's method. This was thought to be due primarily to the errors in measuring the derivatives of the weight loss, used in Friedman's method.

In this work the kinetic parameters were calculated based on data which represented 75% of the total weight loss for H41D and 68% for H41NE. This resulted in large values of the order of reaction and pre-exponential factor for the first region. However, Friedman's results would have been similar to these had he considered the same range of decomposition.

In order to evaluate the effect of separating the reaction into two parts, the thermograms were calculated for H41D using only the kinetic parameters for $W/W_0 \leq 0.89$. This corresponded approximately to the region of weight loss considered by Friedman. As shown by the broken lines in Fig. 6, the calculated vs. experimental thermograms are in poor agreement.

By separating the reaction in this manner, the reaction order and pre-exponential factor become empirical parameters which provide a "best fit" of the data. However, this method yields an extremely accurate reproduction of the thermograms over a wide range of heating rates. This is the desired result for kinetic parameters used in thermal models.

REFERENCES

- 1 H.L. Friedman, *J. Polym. Sci., Part C*, 6 (1965) 183.
- 2 J.H. Flynn and L.A. Wall, *Polym. Lett.*, 4 (1966) 323.

- 3 E.S. Freeman and B. Carroll, *J. Phys. Chem.*, 62 (1958) 394.
- 4 D.A. Anderson and E.S. Freeman, *J. Polym. Sci.*, 54 (1961) 253.
- 5 R.W. Mickelson and I.N. Einhorn, *Thermochim. Acta*, 1 (1970) 147.
- 6 A.D. Baer, J.H. Hedges, J.D. Seader, K.M. Jayakar and L.H. Wojcik, *AIAA J.*, 15 (1977) 1398.
- 7 N.W. Burningham and J.D. Seader, *Thermochim. Acta*, 5 (1972) 59.
- 8 I.J. Goldfarb, R. McGuchan and A.D. Meeks, Air Force Materials Laboratory Technical Report AFML-TR-68-181, Wright-Patterson, Air Force Base, Ohio, 1968.
- 9 S.D. Norem, M.J. O'Niell and A.P. Gray, *Thermochim. Acta*, 1 (1970) 29.